Scaling laws for critical manifolds in polycrystalline materials

J. H. Meinke, E. S. McGarrity, and P. M. Duxbury*
Department of Physics & Astronomy and Center for Fundamental Materials Research, Michigan State University, East Lansing, Michigan 48824-1116, USA

E. A. Holm
Theoretical and Computational Materials Modeling Department, Sandia National Laboratories, Albuquerque, New Mexico 87185-1405, USA

(Received 17 July 2003; published 17 December 2003)

We study the surfaces of lowest energy through model polycrystalline materials in two and three dimensions. When the grain boundaries are sufficiently weak, these critical manifolds (CM's) lie entirely on grain boundaries, while when the grain boundaries are strong, cleavage occurs. A scaling theory for the intergranular to transgranular transition of CM's is developed. The key parameters are the average grain size g, the ratio of grain boundary to the grain interior energy, ϵ, and the sample size L. The key result is that a critical length scale exists, $L_c(g,\epsilon)$, so that on short length scales $l<L_c$ cleavage is observed while at long length scales, $l>L_c$, the critical manifold is rough. We develop a scaling theory for L_c and find that in two dimensions $L_c \approx g x^{y_2}$, while in three dimensions $L_c \approx g \exp(b x^{y_3})$, where $x=\epsilon/(1-\epsilon)$ and b is a constant. Data from realistic polycrystalline grain structures are used to test the scaling theory. The exact lowest energy surface through model grain structures is found using a mapping to the minimum-cut/maximum-flow problem in computer science. As a function of grain-boundary energy, we observe the crossover from grain-boundary rupture to mixed mode failure (a mixture of transgramular and intergranular modes) and finally cleavage and that the two-dimensional data are consistent with $y_2 \approx 3.0 \pm 0.3$, while the three-dimensional data are more difficult to analyze, but are consistent with $y_3 \approx 3.5 \pm 1.0$.

DOI: 10.1103/PhysRevE.68.066107 PACS number(s): 62.20.Mk, 05.10.−a

I. INTRODUCTION

Strongly nonlinear processes in disordered materials frequently lead to the emergence of special manifolds on which current, voltage, stress, or strain localize. Prominent examples of these critical manifolds are fracture surfaces and dielectric trees. These examples arise due to irreversible processes and the critical manifold corresponds to manifolds of damage or rupture. Critical manifolds also emerge in reversible nonlinear processes, such as the localization of current in polycrystalline varistors and the localization of voltage in ceramic superconductors and in Josephson Junction arrays. The manifolds which emerge in these processes have been related to the domain walls which occur in random networks and random Ising magnets [1]. The objective of this contribution is to describe this type of manifold in polycrystalline materials. This problem is interesting from a statistical physics viewpoint as polycrystalline materials are topologically disordered and we would like to know if the scaling laws found for the random bond Ising model extend to this case. This problem is also interesting from a material science viewpoint as a great deal of effort is directed at the engineering of grain-boundary morphology to improve the properties of polycrystalline ceramics and metals [2,3]. To carry out this grain-boundary engineering (GBE), it is necessary to have a relation between the properties of individual grain boundaries along with the cooperative geometry of polycrystalline aggregates and material performance. In many cases, the percolation of special or random boundaries is used as an indicator of material performance. However in the highly nonlinear processes discussed above, the properties of critical manifolds (CM's) as a function of GBE is better indicator of performance. In this contribution we provide the analytic and numerical tools upon which CM analysis of GBE materials is based, while the specific applications to GBE materials will be discussed elsewhere.

The morphology and energy of crystal surfaces have been analyzed using atomistic methods, as have misoriented interfaces between two single crystals [4,5]. However the analysis of critical manifolds requires the study of many thousands of grains and is an important example of a multiscale problem. Atomistic simulations may provide the energy and morphology of an individual grain-boundary, however a higher level, coarse grained, calculation is required to find the energy of separation of a polycrystalline aggregate. In order to carry out this higher level calculation, we develop a graph representation of a polycrystalline aggregate. Each bond in the graph is assigned an energy, which depends on whether it is in the interior of a grain or on a grain-boundary. The model grain structures that we use are generated using the Potts model of grain growth [6,7]. These models reproduce the grain-boundary topology and grain size statistics of metals and ceramics quite accurately.

Finding the lowest energy surface through a graph is a difficult problem, and maps to the problem of finding the lowest energy domain wall in an Ising magnet [8–10]. It is a problem that has many metastable states, so that approaches such as simulated annealing or genetic algorithms cannot guarantee success. There is, however, an efficient method to

*Electronic address: duxbury@pa.msu.edu

find the exact lowest energy surface in a graph. The method is based on a well-known problem from combinatorial optimization, the minimum-cut/maximum-flow problem [11]. The minimal energy surface that we are interested in maps to the minimum cut through a capacitated graph, and the energy of the lowest energy interface is equal to the maximum-flow. In two dimensions, the minimum cut corresponds to a path, which may be found using a different optimization method, Dijkstra's method, as recently demonstrated by one of us [12]. Dijkstra's method is even more efficient than the maximum-flow method, however it identifies special paths while the maximum-flow method must be used to find critical surfaces in three dimensions.

The connection between domain walls in Ising magnets and the minimum-cut/maximum-flow problem has led to improved precision in the calculation of the energy, energy fluctuations, and roughness of domain walls in random bond magnets [8,9]. In this paper we extend the scaling theories developed for domain walls to include the topological disorder occurring in polycrystalline materials. We show that the roughening transition of domain walls in Ising magnets corresponds to the transition from cleavage to intergranular failure in polycrystalline materials, and we find detailed formulas for the behavior of the crossover length as a function of average grain size and grain-boundary energy. The theory we derive is based on those developed for domain walls in random bond Ising magnets [13,14], and their extension to describe periodic elastic media [15–17].

One application of our analysis is to the study of fracture surfaces [18]. The experimental evidence suggests that fracture surfaces have a surface roughness w, which scales as $w \sim L^{\zeta}$, where L is the size of the system and the roughness exponent is found to be in the range $0.5 \leqslant \zeta \leqslant 0.85$. It has been suggested that at short length scales, the ''quasistatic'' exponent should apply [18,19]. We have shown that for mode III failure (or scalar quasistatic failure) this exponent is close to 0.41 [19] in three dimensions. Many of the experiments, however, are carried out in polycrystalline materials, so it is important to test the effect of polycrystalline morphology on the quasistatic exponents. For the case of weak grain boundaries in two-dimensional systems, the intergranular interface problem was recently simulated [12] and it was found that the ball and spring model [20,21] produces surfaces that have similar properties to the minimum surface energy. A second application is to the emergence of voltage manifolds in ceramic superconductors [1,22] and disordered Josephson junction arrays [23]. In these examples, the onset of a measurable macroscopic voltage at the critical current is associated with the emergence of a localized manifold across which the observed voltage drop occurs [1].

Although the model we describe here is idealized it is useful to estimate typical values of the parameter ϵ to be expected in applications. In the application to superconductors, it is known that the critical current of high angle grain boundaries is of order 100 times smaller than the critical current of low angle boundaries. In that case the appropriate ratio is $\epsilon \sim 1/100$ and for isotropic grain structures, the primary failure mode is intergranular. In high T_c materials such as BSCCO, this is mitigated by preparing microstructures with highly elongated grains oriented along the direction of current flow. In applications to structural materials, low angle grain boundaries are 5–10 times better than high angle grain boundaries, so again the failure mode is predominantly intergranular, in the case of uncorrelated random grain boundaries. However in both the superconductor and structural material applications the microstructure may be engineered so as to increase the fraction of low angle grain boundaries. When the fraction of low angle boundaries is high enough, the properties of a material can improve quite dramatically, in a way reminiscent of a percolation process. Generalizations of the theory and models described here may be used to model this effect and will be described elsewhere.

The paper is arranged as follows. In the following section we describe the model that we use. Section III covers the scaling behavior in the limit of weak grain boundaries, while Sec. IV describes the theory for the strong grain-boundary, or cleavage, limit. Section V considers the transition, or mixed-mode, regime which lies between the weak and strong grain-boundary adhesion limits. As in the random manifold and periodic elastic media cases, minimum energy surfaces in polycrystalline systems in both two and three dimensions are always rough in the large lattice limit. Roughening occurs on length scales larger than a critical length L_c which is a function of grain size and grain-boundary energy. Section V focuses on the derivation of expressions for L_c and numerical results to test the predictions. Section VI contains a summary.

II. THE MODEL AND NUMERICAL METHODS

Examples of minimal energy surfaces in polycrystalline microstructures in two and three dimensions are presented in Figs. 1 and 2. The grain structures are grown using an algorithm developed by one of us (E.H.) and described in detail elsewhere [6,7,24]. In brief, a high temperature configuration of a q-state Potts model is quenched to zero temperature. Grains having spin values ranging from 1 to q grow and anneal. The average grain size g increases with time as $t^{1/2}$ in both two and three dimensions, and there is a steady state distribution of grain sizes in the long time limit. The underlying lattice used in these simulations is hypercubic. Each site has a spin label, and grain-boundaries occur when adjacent spin labels are distinct. Bonds which join such distinct spins are identified as grain-boundary bonds. In our simulations we used $q=100$ in two dimensions and $q=256$ in three dimensions.

To analyze the interplay between grain structure and minimal energy surface morphology, we assign grain-boundary bonds an energy ϵ_i and bonds which lie in the interior of the grains an energy ϵ_g. The ratio of these energies is a key parameter and we define $\epsilon = \epsilon_i / \epsilon_g$. More refined models would include orientation dependent grain-boundary energies and/or a variety of lattice orientations inside the grains. It is important, however, to first understand the minimal model we use here.

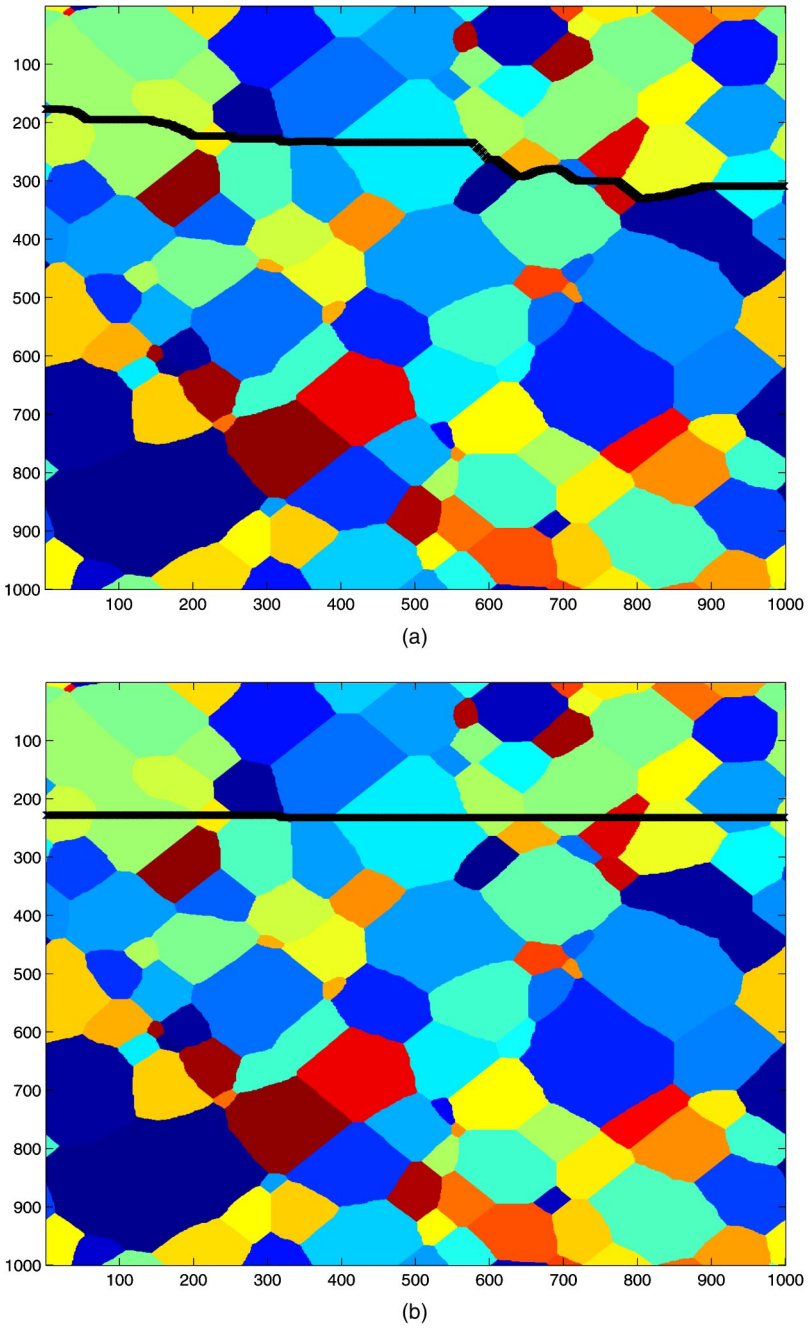

FIG. 1. (Color online) Examples of the lowest energy manifolds in two-dimensional grain structures as a function of the grain-boundary energy (Top, $\epsilon=0.6$, bottom, $\epsilon=0.9$). The sample size is 1000^2.

In order to find the minimal energy surface in our polycrystalline structures, we use a maximum-flow algorithm which we have written in C++. We use the push-relabel algorithm of Goldberg and Tarjan [11] which enables us to find interfaces through 10^6 site systems in about a minute on a high end workstation. We have described the details of this method elsewhere [10].

III. WEAK ADHESION LIMIT $\epsilon \to 0$

In the limit of weak grain-boundary adhesion ($\epsilon \to 0$), the minimal energy surface through a polycrystalline material follows the grain boundaries. The scaling laws for the interface energy and the interface roughness are found by extending the theory developed for random bond-Ising domain walls [13,14]. An example of a random manifold is a minimal energy domain wall in a hypercubic Ising magnet where the exchange constants are all ferromagnetic, but random. There is a well-developed theory for this problem [13,14]. The domain wall is assumed to be described by a single valued height variable $h(r)$, and the scaling predictions for its properties are as follows. The energy of the lowest energy domain wall, E, scales as $E=a_1L^{d-1}+a_2L^{\theta}$, where θ is a universal exponent with $\theta=1/3$ in two dimensions and $\theta=0.82(2)$ in three dimensions [8,9]. L is the system size and a_1 and a_2 are nonuniversal parameters that are dependent on the disorder, but not on the system size. The roughness of the lowest energy domain wall is defined to be $w=\sqrt{\langle h^2\rangle-\langle h\rangle^2}$. The roughness is found to scale as $w=b_1L^{\zeta}$ where $\zeta=2/3$ in two and $\zeta=0.41(1)$ in three dimen-

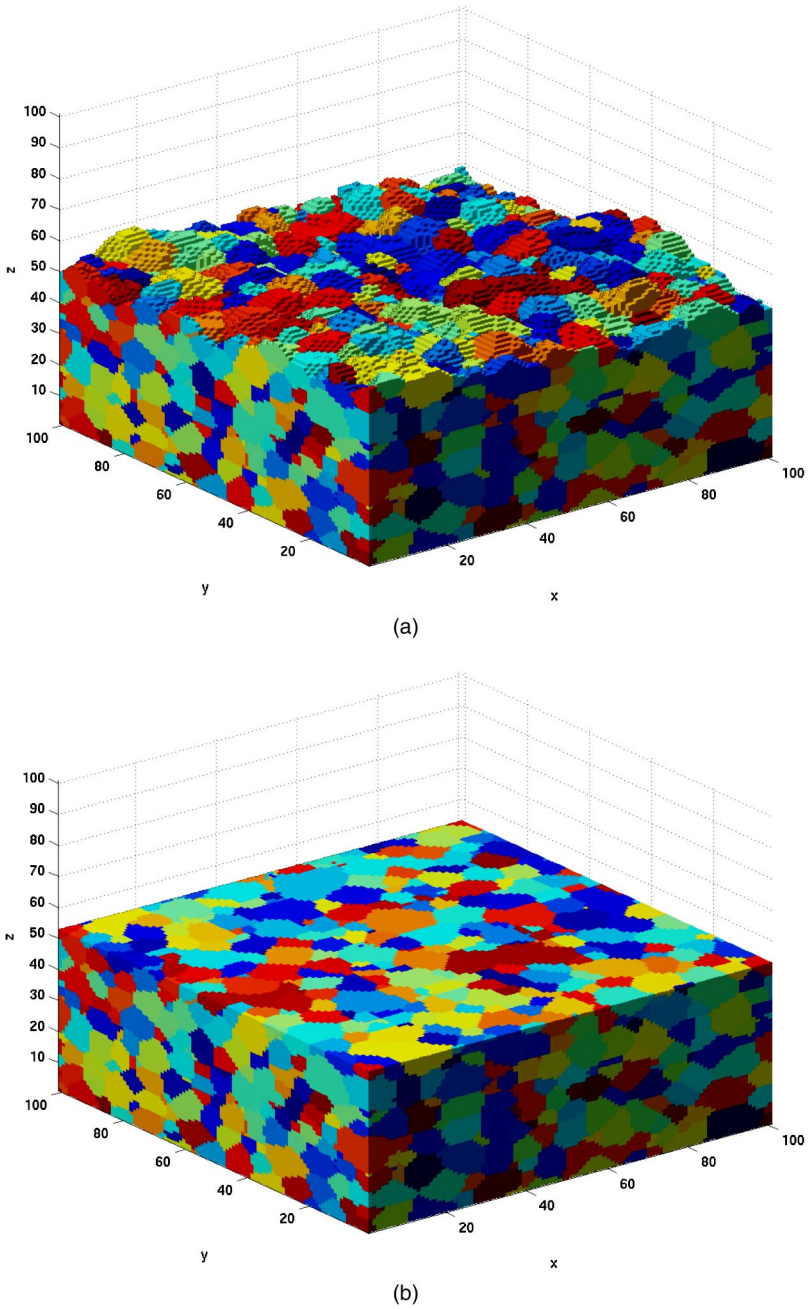

FIG. 2. (Color online) Examples of the lowest energy manifolds in three-dimensional grain structures as a function of the grain-boundary energy. The top figure is for $\epsilon=0.1$, while the bottom figure is for $\epsilon=0.7$. The sample size is 100^3.

sions, and b_1 is a nonuniversal parameter. Note that ζ and θ are universal exponents which do not depend on the details of the disorder or the lattice structure, though they do depend on the spatial dimension. Quantities that are not usually treated, but that are of interest in applications, are the following: the number of bonds on the minimal surface, N, which scales as $N=c_1L^{d-1}+c_2L^{\theta}$; and the fraction of the interface that lies on the grain boundaries, f_i. Here c_1 and c_2 are nonuniversal parameters. If $f_i=1$ the CM is purely intergranular while if $0<f_i<1$, the rupture has a cleavage component.

We extend the scaling laws for random bond Ising domain walls to the case of interest here. We find that the *average grain size acts like a effective lattice constant* so that L/g becomes the effective system size. The scaling law for the energy of a CM is then given by

$$E=g^{d-1}\left[a_1\left(\frac{L}{g}\right)^{d-1}+a_2\left(\frac{L}{g}\right)^{\theta}\right], \tag{1}$$

while the roughness scales as

$$w=b_1g\left(\frac{L}{g}\right)^{\zeta}. \tag{2}$$

In Fig. 3, we see that both relations (1) and (2) are in good agreement with the numerical data. The scaled energy E/L^{d-1} is independent of grain size in both two and three dimensions, indicating that the correction to scaling term involving the L^{θ} term is small compared to the leading term.

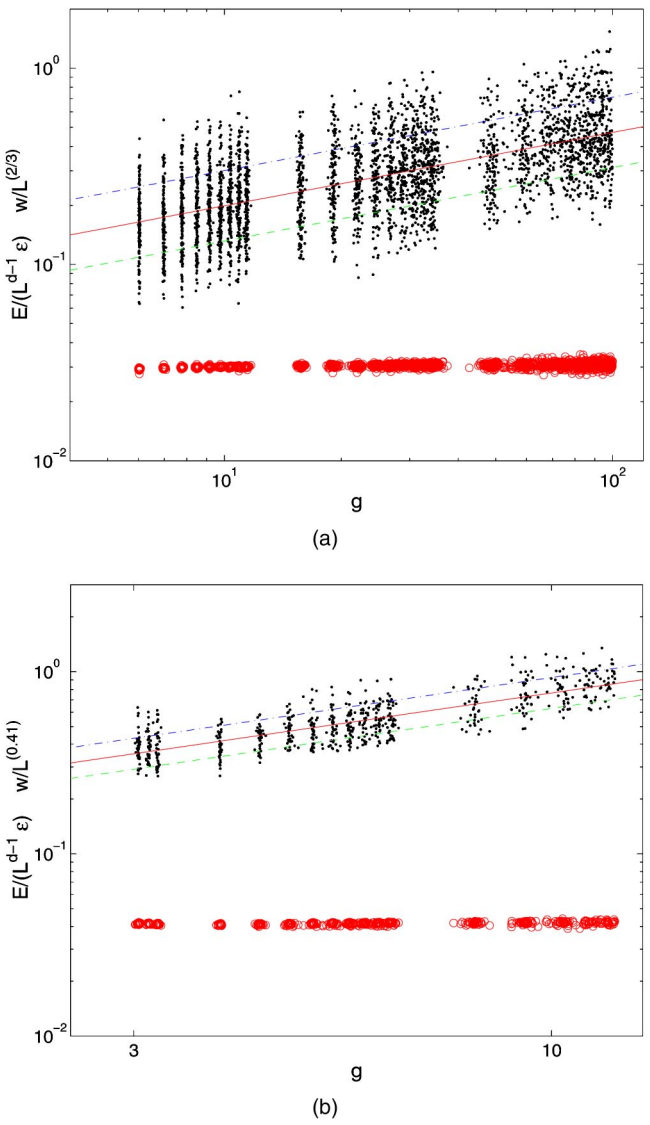

FIG. 3. Tests of the hypothesis that L/g is the effective lattice size. The top figure is for square lattices, while the lower figure is for cubic lattices. If the scaling hypothesis is correct, then $E \sim L^{d-1}$, *asymptotically independent of* g, while $w \sim L^{\zeta} g^{1-\zeta}$. The scaled manifold energy (E/L^{d-1}) as a function of grain size is given by the open circles, while the solid scattered dots give the data for the scaled roughness $(w/L^{\zeta} \sim g^{1-\zeta})$ as a function of grain size. The raw data are plotted for a range of sample sizes varying from $L=500$ to 2000 in two dimensions and $L=50$ to 125 in three dimensions. The fit slopes found, i.e., for the square lattice case (dotted line in the top figure) -0.37 ± 0.05 and for the cubic lattice case (dotted line in the bottom figure) -0.64 ± 0.10, are in good agreement with the scaling prediction $1-\zeta$, which predicts 1/3 in two dimensions and 0.59 ± 0.01 in three dimensions.

The scaled width w/L^{ζ} is found, approximately, to scale as $g^{1-\zeta}$ with $\zeta=2/3$ in two dimensions and $\zeta=0.41(1)$ in three dimensions, in nice agreement with the scaling predictions.

In the weak grain-boundary limit, the manifold energy is proportional to the number of bonds N in the interface,

$$E = \epsilon_g \epsilon N \tag{3}$$

and N must therefore scale like the energy,

$$N = g^{d-1}\left[c_1\left(\frac{L}{g}\right)^{d-1} + c_2\left(\frac{L}{g}\right)^{\theta}\right].$$

As we shall see in Sec. IV, the weak adhesion limit applies over quite a broad range of grain-boundary energies, with a mixed transgranular and intergranular failure regime setting in at $\epsilon_c \approx 1/2$ in two dimensions and $\epsilon_c \approx 1/3$ in three dimensions. However, these thresholds are nonuniversal and should be expected to depend on the details of the grain structure and lattice geometry.

In the simulations described here there is an underlying square or cubic lattice. The critical value of ϵ can be estimated by considering the conditions under which the interface prefers to cleave a section of the grain containing two atoms (square lattice) or a two-atom square (cubic lattice). We choose these configurations as a study of the grain structures indicates that they are the smallest facets which appear frequently in the polycrystalline microstructure. The energy to cleave two atoms on a square lattice is $2\epsilon_g$, and that required to cleave a two-atom square on a cubic lattice is $4\epsilon_g$. The energy to follow the grain-boundary is $4\epsilon_i$ (square lattice) and $12\epsilon_i$ (cubic lattice). Balancing these two energies leads to the critical values $\epsilon_c=1/2$ (square) and $\epsilon_c=1/3$ (cubic). These values are quite close to the thresholds seen in the simulations (see Figs. 4–7), though in simulations the threshold is not sharp, as other local configurations play a role in determining the threshold.

IV. STRONG ADHESION LIMIT

The strong adhesion limit applies only in the limit $\epsilon \to 1$. Nevertheless it is useful to understand this limit to set the stage for the mixed regime $\epsilon_c \leqslant \epsilon < 1$. When cleavage occurs, i.e., the interface is flat. The roughness and number of bonds are $w=0$ and $N=L^{d-1}$, respectively. The energy can be expressed as $E=\epsilon_g(f_g+\epsilon f_i)$, where f_g is the fraction of the interface within the grain, f_i is the fraction of the interface along grain boundaries, and $f_g+f_i=1$. We can rewrite the energy in terms of f_i:

$$E = \epsilon_g(1 - f_i + \epsilon f_i). \tag{4}$$

Note that f_i is *not* zero even in the cleavage limit, as even a flat surface must cross some grain boundaries. As can be seen from Eq. (4) the energy is proportional to ϵ as long as f_i is a constant, which is true provided the interface does not begin to roughen.

In the limit of a cleavage surface a simple argument for f_i can be made, which turns out to be wrong for our grain structures but which is useful nevertheless. The interface has to cross on average L^{d-1}/g^{d-1} grains. The area of the grain-boundary of each crossing is proportional to g^{d-2} and the total area of the interface is L^{d-1}. The fraction of the interface along grain boundaries is then

$$f_i = d_1 \frac{g^{d-2} L^{d-1}}{L^{d-1} g^{d-1}} = d_1 \frac{1}{g}, \tag{5}$$

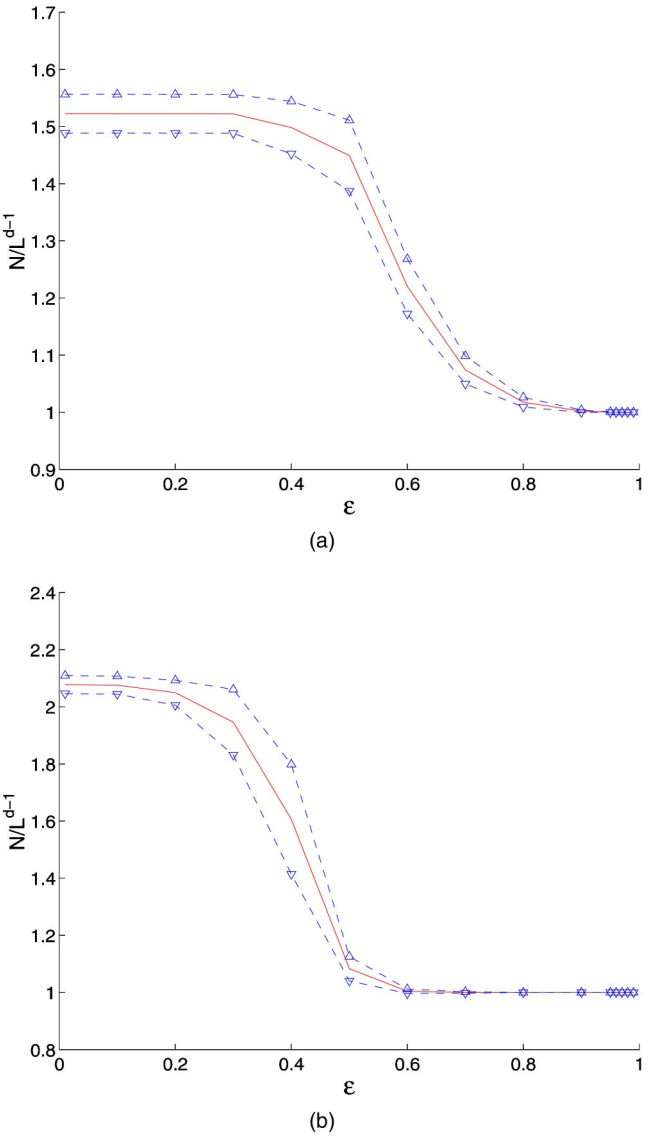

FIG. 4. The total number of bonds which cross the critical manifold. The top figure is for two dimensional grain structures, while the bottom figure is for three-dimensional grain structures. The solid line is the average, while the dashed lines indicate one standard deviation in the data. The calculations are for the following values of sample size L (and number of configurations N). For square lattices 500(51), 1000(54), 1200(20), 2000(2), with the average grain size g varying from 6 to 100; for cubic lattices we used $L(N)=50(10)$, 75(10), 100(10), 125(10), with the grain size in the interval, $3\leqslant g\leqslant 12$.

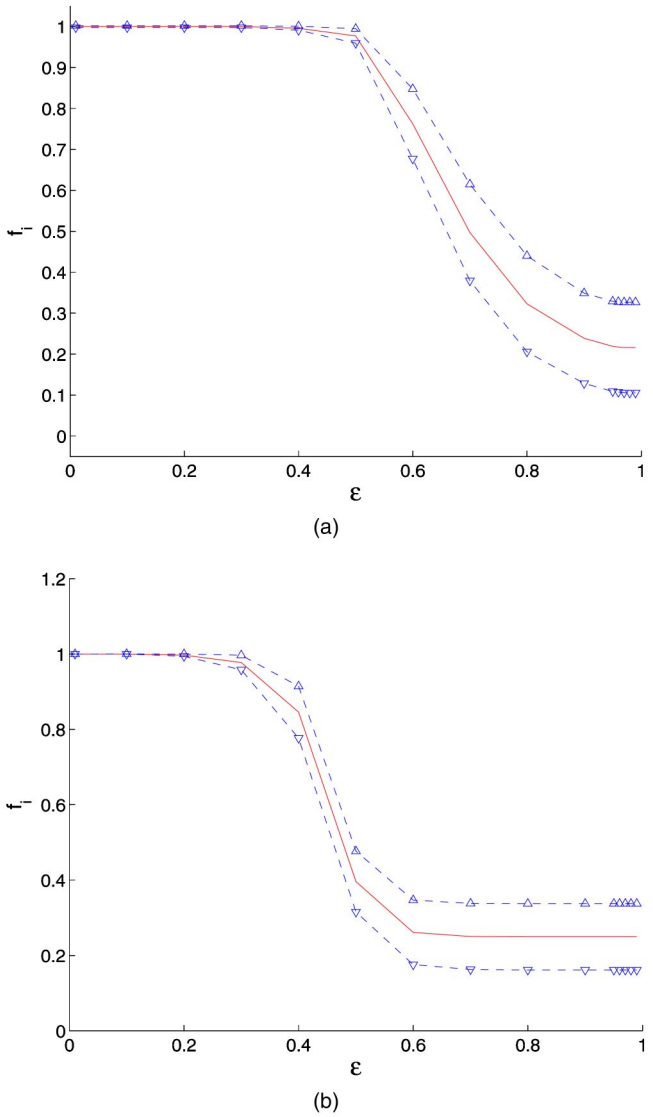

FIG. 5. The fraction of the CM, f_i, which is composed of grain-boundary bonds. The top figure is for two-dimensional systems, while the bottom figure is for three-dimensional systems. The solid line is the average, while the dashed lines indicate one standard deviation in the data. The sample size, number of configurations, and grain sizes used are the same as those given in the caption to Fig. 4.

where d_1 is a constant that depends on the details of the grain-boundary structure, but is independent of the average grain size g. However Eq. (5) does not describe the data well. Instead, f_i seems to be quite insensitive to variations in grain size. This may be understood as being due to facets. For any $\epsilon<1$, it is energetically favorable to maximize the number of grain-boundary bonds on the CM, and in a faceted microstructure, this is achieved by placing the cleavage surface on the plane with the maximum number of facets. This effect is not taken into account in the estimate, Eq. (5). In a system with near spherical grains, however, we would expect Eq. (5) to hold.

V. INTERMEDIATE REGIME

Results found from analysis of interfaces in polycrystalline materials as a function of the grain-boundary bond strength ϵ are presented in Figs. 4–7. It is seen from this data that the weak adhesion behavior persists up to energy ratios $\epsilon_c\sim 1/2$ in two dimensions and $\epsilon_c\sim 1/3$ in three dimensions. At higher grain-boundary adhesion, we enter the mixed regime, where the fraction of the interface which is intragranular is a sensitive function of the adhesion energy ϵ. In two dimensions, the mixed phase persists up to $\epsilon\sim 0.92$; however,

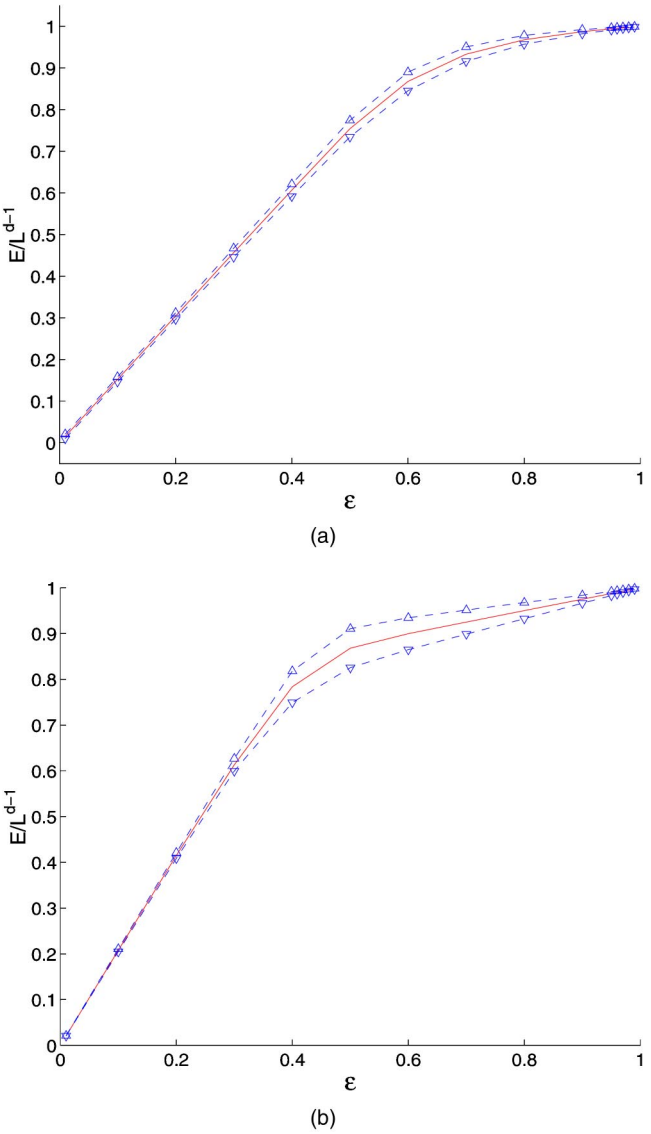

FIG. 6. Average interface energy (solid line) per unit area and its standard deviation (up and down triangles) vs ϵ. The top figure is for two-dimensional grain structures, while the bottom figure is for three-dimensional grain structures. The sample size, number of configurations and grain sizes used are the same as those given in the caption to Fig. 4.

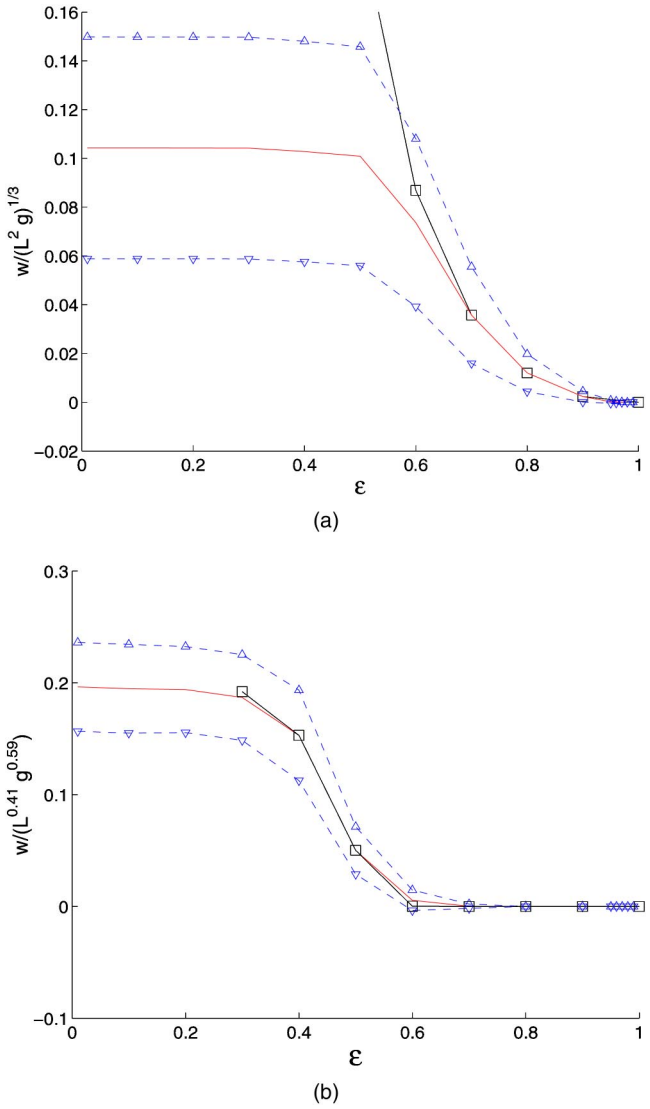

FIG. 7. The scaled interface width $w/(L^{\zeta}g^{1-\zeta})$ vs ϵ. The top figure is for two-dimensional grains structures, while the bottom figure is for three-dimensional grain structures. The solid line which joins the square symbols is a fit to Eq. (19) (top figure) and Eq. (20), with $y_3=4$ (bottom figure). The solid line which extends over the entire ϵ range is the average of the data, while the dashed lines indicate one standard deviation. The sample size, number of configurations, and grain sizes used are the same as those given in the caption to Fig. 4.

in three dimensions cleavage sets in at $\epsilon \sim 0.70$. However, we argue, based on an understanding of similar issues in models of periodic elastic media, that in reality CM's are rough for $\epsilon > 0.7$, provided the sample size $L > L_c$, where L_c is a critical length which diverges exponentially with the energy $1-\epsilon$. This means that cleavage occurs on short length scales, but that on long enough length scales CM's in three dimensions are rough. We now present an analytic argument to describe the way in which the crossover from cleavage to intergranular failure occurs in the mixed phase.

Our theory for the onset of the mixed rupture regime is based on theories for the roughening of manifolds in periodic elastic media [15–17]. The key idea originated with Imry and Ma [25] who constructed a theory for the instability of the ferromagnetic phase in the random-field Ising model. In the case of critical manifolds in polycrystalline materials, for any $\epsilon < 1$ there is a competition between the reduction in energy produced when the interface incorporates boundary bonds and the extra bonds which are caused by any deviation from cleavage. The scaling theory is a consequence of finding the manifold which minimizes the sum of these competing energies.

For ease of discussion we first consider faceted grains in two dimensions, as indicated in Fig. 8. In this case, whenever the fracture interface encounters a grain boundary it has two choices. It can either go straight through the grain and cleave it or follow one of the available grain-boundary paths. We assume that a grain boundary makes an angle θ with the

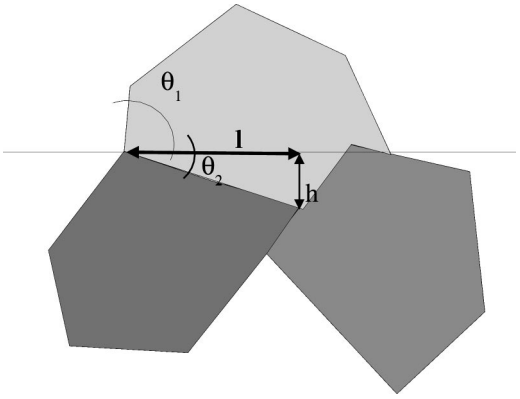

FIG. 8. A manifold through a faceted grain structure.

cleavage interface. The grain-boundary path is longer than the cleavage path, which has a length l. The length of the grain-boundary facet is then $l+h$, due to the underlying square lattice. The grain-boundary angle is related to h and l by, $\theta=\arctan(h/l)$. For a given value of grain-boundary energy ϵ, there is a critical grain-boundary angle above which cleavage occurs. The condition for this critical angle is

$$\frac{\epsilon(l+h)}{l} \geqslant 1,$$

$$\frac{h}{l} \geqslant \frac{1}{\epsilon} - 1,$$

which gives the critical angle for a given ϵ

$$\theta_c = \arctan\left(\frac{1}{\epsilon} - 1\right). \tag{6}$$

It is locally favorable for the critical manifold to follow all grain-boundary facets with angles θ smaller than θ_c.

The argument above gives the *local* picture of how the interface roughens. According to this local picture, the local fraction f_L of grain boundaries which lie on a minimal energy surface is given by

$$f_L = \int_{-\theta_c}^{\theta_c} P(\theta)\, d\theta, \tag{7}$$

where $P(\theta)$ is the probability that a grain-boundary is at angle θ to the cleavage direction. In the case of randomly oriented grains, $P(\theta)$ is a constant, so we have

$$f_L \approx A\theta_c \approx \frac{1-\epsilon}{\epsilon}, \tag{8}$$

where A is a normalization constant. In the last expression on the right-hand side of Eq. (8), we have used a linear expansion of the arctan function. In three dimensions the arguments are more complex; however, for the arguments below, we only need to define a local fraction f_L. A refinement which may be important in some cases is to include the curvature of the grain boundaries. If curvature is included, the grain boundaries may partially fail. In the three-dimensional case partial failure is also more likely. However, this does not qualitatively change the analysis, so for ease of discussion we derive the basic results assuming only complete rupture of facets.

The argument above describes the local variations in the CM morphology. However, we seek the *global minimum* energy surface. To find the global minimum we need to consider the energy fluctuations on large length scales. On large length scales, there exist statistically favorable regions where a number of small angle facets are close to each other. It is energetically favorable to include these regions in the minimum energy interface. To include these favorable regions, it is necessary for the interface to roughen. The interplay between the desire of the interface to accommodate favorable regions with many low angle facets and the energy cost of manifold wandering determines the interface roughness. We now make this energy balance quantitative.

According to the local argument, culminating in Eq. (8), the typical number of facets which occur due to local deviations from a cleavage surface is given by

$$N_f = f_L (L/g)^{d-1}. \tag{9}$$

The central limit theorem states that the typical variation in this quantity is $\delta N_f = N_f^{1/2}$. Such variations can be either positive (unfavorable fluctuations) or negative (favorable fluctuations). In our case, the favorable case corresponds to a clustering of grain boundaries which have low angles to the cleavage direction. There is another factor which must be considered, and that is the fact that there are many ways in which a favorable fluctuation on an interface may be selected, that is, the minimal energy fluctuations may occur in many different places in the material. This is an entropylike factor. The typical number of ways that the set N_f of facets may be selected on a cleavage plane is of order (L/g). To include this factor in estimating the typical largest energy gain, we set

$$\frac{L}{g} e^{-\delta N_f^2 / N_f} \approx 1. \tag{10}$$

This sort of argument has been used in other rare fluctuation problems, for example, in estimating the fracture strength of random networks [26]. The typical size of the most favorable fluctuation in the number of low angle facets in a minimal energy surface is then

$$\delta N_{f,max} \approx f_L^{1/2} \left(\frac{L}{g}\right)^{(d-1)/2} \left[\ln\left(\frac{L}{g}\right)\right]^{1/2}. \tag{11}$$

The typical energy gain for each favorable facet is $\epsilon_g(1-\epsilon)g^{d-1}/2$. Multiplying this by the typical largest favorable fluctuation in the number of facets [Eq. (11)] gives

$$U_{\text{gain}} \approx -\epsilon_g (1-\epsilon) g^{d-1} f_L^{1/2} \left(\frac{L}{g}\right)^{(d-1)/2} \left[\ln\left(\frac{L}{g}\right)\right]^{1/2}, \tag{12}$$

where we have dropped constant factors. To take advantage of this energy gain, the interface must make excursions from

the cleavage plane which are of the order of the grain size. This leads to an energy cost of order

$$U_{\mathrm{cost}} \approx \epsilon_g \epsilon \; g L^{d-2}.$$

Setting $U_{\mathrm{gain}} + U_{\mathrm{cost}} = 0$ we find a relation between the critical length L_c, the grain size, and the grain-boundary adhesion,

$$\frac{1-\epsilon}{\epsilon} = \frac{B\left(\frac{L_c}{g}\right)^{(d-3)/2}}{f_L^{1/2}\left[\ln\left(\frac{L_c}{g}\right)\right]^{1/2}}. \tag{13}$$

Here B is an undetermined constant, which depends on the details of the grain structure, lattice structure, etc. In two dimensions Eq. (13) becomes

$$\frac{1-\epsilon}{\epsilon} = \frac{B}{f_L^{1/2}\left(\frac{L_c}{g}\right)^{1/2}\left[\ln\left(\frac{L_c}{g}\right)\right]^{1/2}} \tag{14}$$

while in three dimensions we find

$$\frac{1-\epsilon}{\epsilon} = \frac{B}{f_L^{1/2}\left[\ln\left(\frac{L_c}{g}\right)\right]^{1/2}}. \tag{15}$$

From Eqs. (14) and (15) we can conclude that for large enough systems the cleavage state is unstable to fluctuations for *any* $\epsilon < 1$ in both two and three dimensions. This is most easily understood by isolating the critical length. In two dimensions, the logarithmic term in Eq. (14) is usually negligible, in which case we find that the critical length is given by, after dropping constant terms,

$$L_c = \frac{g}{f_L}\frac{\epsilon^2}{(1-\epsilon)^2} \approx g\left(\frac{\epsilon}{1-\epsilon}\right)^{y_2}, \tag{16}$$

where the last expression on the right-hand side of this equation is found by using Eq. (8), which also implies that $y_2 = 3.0$. In three dimensions, the logarithm is important and it leads to a critical length which is an exponential function of the grain-boundary adhesion. From Eq. (15) we have

$$L_c = g\exp\left(\frac{1}{f_L}\frac{(B\epsilon)^2}{(1-\epsilon)^2}\right) \approx g\,\exp\left[b\left(\frac{\epsilon}{1-\epsilon}\right)^{y_3}\right], \tag{17}$$

where b is an unknown constant. In writing the last expression in the right-hand side of Eq. (17), we have assumed that $f_L \approx [(1-\epsilon)/\epsilon]^{y_3-2}$ as is implied by Eq. (8), with $y_3 = 3$. However Eq. (8) may not apply to three-dimensional grain structures, where partial failure of facets is likely, so in analyzing the data, we allow y_3 to be a free parameter.

For sample sizes $L < L_c$ the CM's have constant roughness, while for sample sizes $L > L_c$ the interface roughness grows as $(L/L_c)^{\zeta}$ with increasing length scale. L_c is also the linear size of the cleavage regions on the interface. These cleavage regions are terminated by steps which are of the order of grain size. Critical manifolds are thus flat on length scales less than L_c and algebraically rough on larger length scales. The critical length diverges as $\epsilon \to 1$ and decreases continuously with decreasing $\epsilon < 1$. At the transition point to the weak adhesion limit (which occurs at $\epsilon_c \sim 1/d$), where d is dimension, it becomes a constant and $L_c = g$. Formulas (16) and (17) are valid up to the transition to the weak adhesion limit.

L_c is exponentially dependent on $\epsilon/(1-\epsilon)$ in three dimensions and only algebraically dependent on this quantity in two dimensions. This means that L_c diverges very rapidly as $\epsilon \to 1$ in three dimensions so that cleavage is typical for ϵ near one, even in large samples. This is illustrated in Fig. 9,

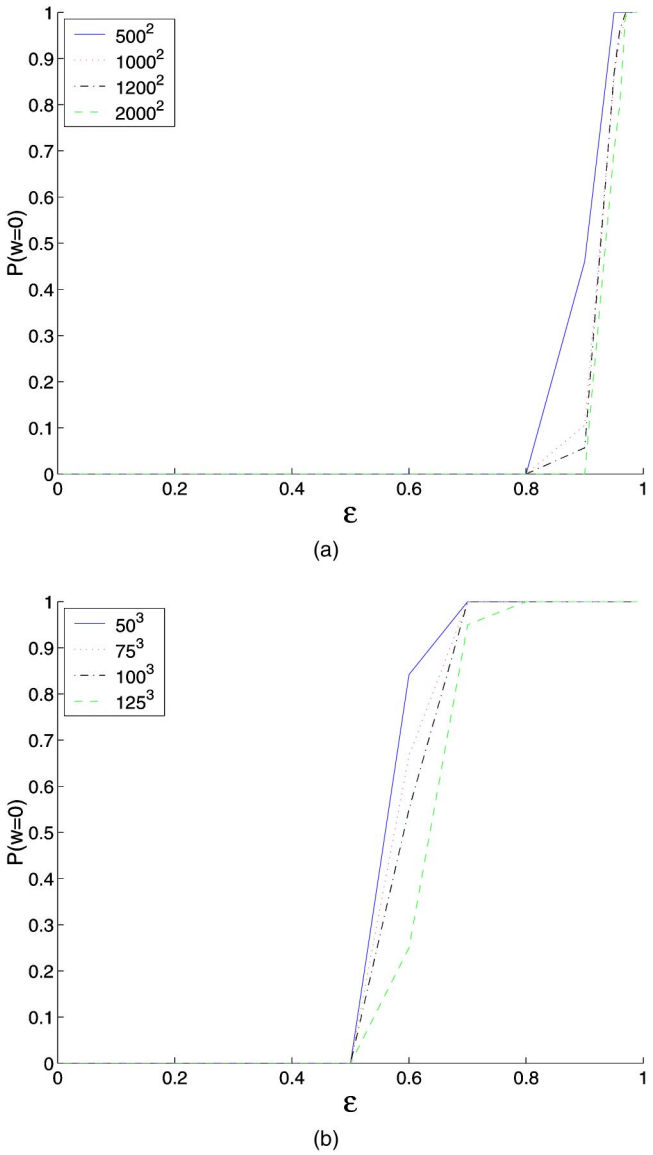

FIG. 9. The probability that a critical manifold has zero roughness as a function of ϵ. The upper figure is for square lattices, while the lower figure is for cubic lattices. The sample size is given in the legend to each figure. The grain sizes used for the square lattice case are restricted to $g \approx 9.5$, while in the three-dimensional case $g \approx 6.5$.

which gives the probability that cleavage occurs as a function of ϵ. For the sample sizes available to us, cleavage is almost certain for $\epsilon > 0.7$ in three dimensions, while in two dimensions mixed mode failure persists for $\epsilon < 0.93$. This is partially due to the larger sample sizes available in two dimensions, but it is mostly due to the exponential divergence in L_c in three dimensions.

In order to test the scaling predictions for L_c, we rewrite the scaling behavior of the roughness in terms of L_c,

$$\frac{w}{g} \approx \left(\frac{L}{L_c} \right)^{\zeta}. \tag{18}$$

Using this formula, we should be able to collapse data for different values of g and ϵ onto one scaling plot. However, this data collapse can only be expected in a range of $\epsilon > \epsilon_c$ and up to the value of ϵ at which cleavage becomes most likely. For the sample sizes available to us, this restricts the value of ϵ that we can use to quite a narrow range. The results are nevertheless quite good, as seen in Fig. 10. The scatter in the data is real, there are strong variations in the roughness even in the case of intergranular rupture (see Fig. 3). From this analysis we find that the theoretical prediction, Eq. (16), with $y_2 = 3$ is well supported by the data. The three-dimensional data are less restrictive and we are only able to state that the data are consistent with Eq. (17), with $y_3 \approx 3.5 \pm 1.0$.

From the theory developed above and in Secs. III and IV, it is possible to understand the behavior of the quantities plotted in Figs. 4–7 as a function of the energy ratio ϵ. First consider the width data presented in Fig. 7. In two dimensions, using Eqs. (16) and (18) the theory predicts that

$$\frac{w}{g^{1/3} L^{2/3}} \approx \left(\frac{1-\epsilon}{\epsilon} \right)^2 \tag{19}$$

while in three dimensions Eqs. (17) and (18) imply that

$$\frac{w}{g^{1-\zeta} L^{\zeta}} \approx \exp\left[-b \left(\frac{\epsilon}{1-\epsilon} \right)^{y_3} \right], \tag{20}$$

where b is a constant which is not specified by the scaling theory and $y_3 \approx 3.5 \pm 1.0$. The fact that $w \approx 0$ for $\epsilon > 0.7$ is due to the fact that the critical length is very large in three dimensions. Nevertheless, we expect finite roughness in macroscopic samples for all $\epsilon > \epsilon_c \approx 1/d$. The solid lines connecting the boxes in Fig. 7 give fits to Eqs. (19) (top figure in Fig. 7) and (20) (bottom figure in Fig. 7). The fits are very good near $\epsilon = 1$, even in the regime in which the finite samples which we are considering frequently undergo cleavage. The fact that the three-dimensional case fits well even close to the intergranular regime is probably fortuitous. The theory is not strictly valid in that regime.

The energy (see Fig. 6) is a linear function of ϵ for $\epsilon < \epsilon_c$ [see Eq. (3)]. The energy is also a linear function of ϵ when cleavage occurs [see Eq. (4)]. In our three-dimensional samples this occurs for $\epsilon > 0.7$. There is then only a small region (see Fig. 6, bottom figure) in which the energy is a nonlinear function of ϵ. Again in the limit of macroscopic samples the nonlinear regime extends all the way to $\epsilon = 1$, though it should look almost linear due to the exponential behavior of L_c.

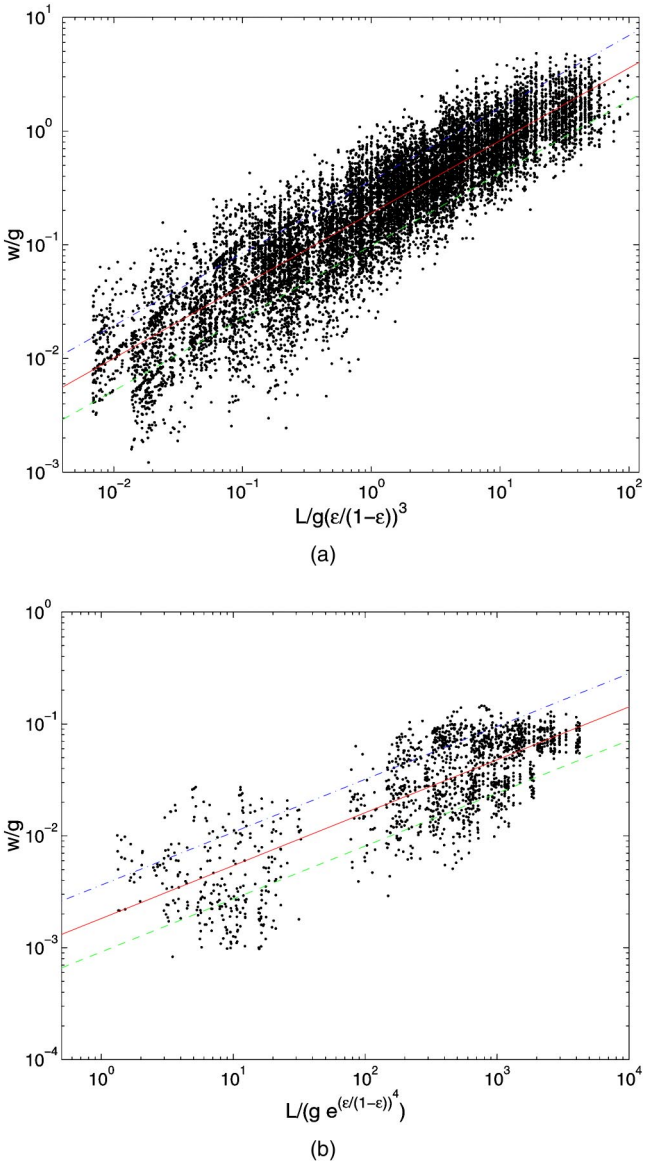

FIG. 10. Scaling of roughness. The roughness w/g is plotted vs L/L_c on a log-log scale. We used the same number of configurations, grain sizes, and configurations as quoted in the caption to Fig. 4. The top figure is for square lattices in the mixed regime $0.6 \leqslant \epsilon \leqslant 0.9$ and we used Eq. (16) for L_c, with $y_2 = 3$. The solid line is a best fit line and has slope 0.64 ± 0.10, which is consistent with the scaling prediction $\zeta = 2/3$ in two dimensions. The bottom figure is for cubic lattices in the mixed regime $0.4 \leqslant \epsilon \leqslant 0.6$ and we used Eq. (17) for L_c, with $y_3 = 4$. The solid line is a best fit line and has slope 0.47 ± 0.10, which is consistent with the scaling prediction $\zeta = 0.41 \pm 0.01$ in three dimensions.

The fraction of CM bonds which are grain-boundary bonds, f_i (see Fig. 5) is approximated by (in two dimensions)

$$f_i = f_L + \frac{g}{g + L_c}, \tag{21}$$

where f_L is the fraction of facets which are energetically favorable, based on a local condition, and the ratio $g/(g+L_c)$ gives the additional interface bonds which occur due to the contribution from nonlocal wandering. In three dimensions the analogous expression is

$$f_i = f_L + \frac{2\pi g L_c}{2\pi g L_c + \pi L_c^2}. \tag{22}$$

Similar expressions can be found for the number of bonds on the interface (Fig. 4). Using Eqs. (19) and (20), these expressions lead to rather complex functions of ϵ; however, the main point to be taken away from the analysis is that the critical length L_c sets the scale for the crossover from intergranular to mixed mode to cleavage in all of the observables that we have studied.

From the analysis above it is clear that once we find L_c as a function of material parameters, it is possible to develop a detailed theory for the behavior of many of the properties of interest as a function of material parameters. In our current work we are developing formulas for L_c in more realistic cases such as GBE materials and in fiber and platelet reinforced materials.

VI. SUMMARY

The energy and morphology of the minimum energy surfaces in polycrystalline materials have been analyzed. These minimum energy surfaces are (CM's) in the sense that they are the surfaces on which voltage localizes in certain nonlinear electrical processes [1], and they provide an approximation to quasistatic fracture surfaces at short distances [18].

We have developed a scaling theory to describe the behavior of the CM energy and interface morphology as a function of the ratio of the grain-boundary energy to the intragrain energy, ϵ. Intergranular processes dominate up to a critical threshold $\epsilon_c \approx 1/d$, for d-dimensional hypercubic lattices. In the mixed mode phase, $\epsilon > \epsilon_c$, the critical manifold is accommodated partially by grain-boundary rupture and partially through cleavage of the grains. We found that on short length scales $l < L_c$ cleavage occurs, but that on long length scales $l \gg L_c$ CM's are always rough in both two and three dimensions. The critical length L_c is simply proportional to the average grain size, but is a more nontrivial function of the energy ratio ϵ. Explicit expressions for L_c are given in Eqs. (16) and (17) for two and three dimensions, respectively. These expressions are confirmed by numerical simulations using the maximum-flow algorithm [see Figs. 4–10). We showed that it is possible to relate the behavior of properties of interest, such as the intergranular fraction f_i and the CM roughness w, to L_c so that L_c is the central quantity of the theory.

We are currently using this approach to study grain-boundary engineered materials where the objective is to increase the number of low angle grain boundaries in order to improve the material performance. In a more general context, it has been realized for some time that it is necessary to develop theories for the performance of complex materials that go beyond the unit cell model [27,28]. In the case of polycrystalline materials, the unit cell model uses the average grain size as the typical length scale. The crossover length L_c introduced here is due to a cooperative effect of many grain boundaries. It provides an interesting new alternative length scale which is important in a broad range of nonlinear effects in polycrystalline materials.

ACKNOWLEDGMENTS

The research at MSU was supported by the DOE under Contract No. DEFG02-90ER45418, and by Sandia National Laboratories. This work was performed in part at Sandia National Laboratories, a multiprogram laboratory operated by Sandia Corporation, a Lockheed Martin Company, for the United States Department of Energy under Contract No. DE-AC04-94AL85000.

[1] A. Donev, C.E. Musolff, and P.M. Duxbury, J. Phys. A **35**, L327 (2002).
[2] T. Watanabe and S. Tsurekawa, Acta Mater. **47**, 4171 (1999).
[3] C.A. Schuh, M. Kumar, and W.E. King, Acta Mater. **51**, 687 (2003).
[4] A. Zangwill, *Physics at Surfaces* (Cambridge University Press, Cambridge, 1988).
[5] A. P. Sutton and R. W. Baluffi, *Interfaces in Crystalline Materials* (Oxford University Press, Oxford, 1995).
[6] D.J. Srolovitz, M.P. Anderson, P.S. Sahni, and G.S. Grest, Acta Metall. **32**, 793 (1984).
[7] M.P. Anderson, D.J. Srolovitz, G. Grest, and P. Shani, Acta Metall. **32**, 783 (1984).
[8] A.A. Middleton, Phys. Rev. E **52**, R3337 (1995).
[9] M.J. Alava and P.M. Duxbury, Phys. Rev. B **54**, 14 990 (1996).
[10] M.J. Alava, P.M. Duxbury, C.F. Moukarzel, and H. Rieger, in *Phase Transistions and Critical Phenomena*, edited by C. Domb and J. Lebowitz (Academic Press, New York, 2001), Vol. 18.
[11] A.V. Goldberg and R.E. Tarjan, J. Assoc. Comput. Mach. **35**, 921 (1988).
[12] E.A. Holm, J. Am. Ceram. Soc. **81**, 455 (1998).
[13] D.A. Huse and C.L. Henley, Phys. Rev. Lett. **54**, 2708 (1985).
[14] D.S. Fisher, Phys. Rev. Lett. **56**, 1964 (1986).
[15] J.P. Bouchaud and A. Georges, Phys. Rev. Lett. **68**, 3908 (1992).
[16] T. Emig and T. Nattermann, Eur. Phys. J. B **8**, 525 (1999).
[17] E.T. Seppälä, M.J. Alava, and P.M. Duxbury, Phys. Rev. E **63**, 036126 (2001).
[18] E. Bouchaud, J. Phys.: Condens. Matter **9**, 4319 (1997).
[19] V.I. Raisanen, E.T. Seppälä, M.J. Alava, and P.M. Duxbury, Phys. Rev. Lett. **80**, 329 (1998).
[20] M. Sahimi and J.D. Goddard, Phys. Rev. B **33**, 7848 (1986).
[21] P.D. Beale and D.J. Srolovitz, Phys. Rev. B **37**, 5500 (1988).

[22] R. Haslinger and R. Joynt, Phys. Rev. B **61**, 4206 (2000).
[23] P.L. Leath and W. Xia, Phys. Rev. B **44**, 9619 (1991).
[24] E.A. Holm and C.C. Battaile, J. Miner., Met. Mater. Soc. **53**, 20 (2001).
[25] Y. Imry and S.K. Ma, Phys. Rev. Lett. **35**, 1399 (1975).
[26] P.M. Duxbury, P.L. Leath, and P.D. Beale, Phys. Rev. B **36**, 367 (1987).
[27] C.S. Nichols, R.F. Cook, D.R. Clarke, and D.A. Smith, Acta Metall. Mater. **39**, 1657 (1991).
[28] C.S. Nichols, R.F. Cook, D.R. Clarke, and D.A. Smith, Acta Metall. Mater. **39**, 1667 (1991).